Investigating the Reason for Compressor Gearbox Gear Failure in Arfa Iron and Steel Company using Analytical and Fracture Studies

Mahdi Ebrahimzadeh
Department of Mechanical Engineering,
Najafabad Branch, Islamic Azad University, Najafabad, Iran
E-mail: m.ebrahimzadeh@smc.iaun.ac.ir

SeyedAli Galehdari*
Department of Mechanical Engineering,
Najafabad Branch, Islamic Azad University, Najafabad, Iran
Modern Manufacturing Technologies Research Center,
E-mail: ali.galehdari@pmc.iaun.ac.ir
*Corresponding author

Received: 19 January 2018, Revised: 12 February 2018, Accepted: 15 April 2018

Abstract: Given the application of gears in various industries including steel industries, studying the reasons for facture in gears before reaching the end of their lifetime is of great importance. In this study, a gearbox was investigated which included a gear and a pinion. After four years of use, the teeth of gear and pinion along with the shaft attached to the gear were fractured. The fracture had occurred suddenly and with a lot of noise. The fracture in gear and pinion were in the teeth while the fracture in shaft occurred in the keyway. At the beginning of the study, shaft and gear design equations were used to evaluate the suitability of each of the parts in the system using theoretical equations and then fracture type was determined using fracture studies and the accuracy of analytical results were determined. In the analytical study, the results showed that the fracture is due to improper design for the gear shaft leading to more than one million unites of load on the shaft leading to cracks in the keyway and misalignment between gears causing fracture. In the fracture studies, the fracture type (ductile and brittle) was determined and the accuracy of analytical results was confirmed. In the numerical results, the distribution of static strain in the fractured shaft and a redesigned shaft are investigated.

Keywords: Design analysis, Fracture studies, Gearbox, Gear failure

Reference: Ebrahimzadeh, Mahdi, Galehdari, SeyedAli, "Investigating the Reason for Compressor Gearbox Gear Failure in Arfa Iron and Steel Company using Analytical and Fracture Studies", Int J of Advanced Design and Manufacturing Technology, Vol. 11/No. 2, 2018, pp. 1-13.

Biographical notes: S.A. Galehdari, received his PhD in Mechanical Engineering from Ferdowsi University of Mashhad in 2015. He is currently Assistant Professor at the Department of Mechanical Engineering, Najafabad University, Najafabad, Iran. His current research interest includes Fracture and Failure analysis. **M. Ebrahimzadeh** is MSc student at the Department of Mechanical Engineering, Islamic Azad University, Najafabad, Iran.

1 INTRODUCTION

Gears are the most important part of rotating equipment and premature gear failure is one of the problems in industries. Investigating the reasons for gear failure and providing methods for reducing these failures can improve the productivity of equipment and performance by reducing premature failure of equipment.

There are various reasons for failure in gears [1]. In this regard, Patel et al., studied general defects in gearboxes [2]. Sometimes the reason for gears' failure is the defective parts attached to them [3]. Therefore, it is important to properly design the shafts which are one of the most important parts attached to gearboxes. In this context, Lan Zeotti et al. [4] studied the spin, shaft and thorn in a rotating machine using scanning electron microscopy. Another important consideration is the selection of materials used to manufacture the gears because using the wrong materials can lead to premature failure. Yusel et al., [5] reviewed the failure of gear wheels of a motor. This paper includes studying the mechanical properties of the material of the ribs and the subsequent process of making them, and investigating the variations in the hardness and vibrations introduced by the nails due to their failure. The selection of proper materials and correct designs are two important steps of designing proper gearboxes [6]. American Caster Association states that failure in gears can be due to 1. Aberration, 2. Surface fatigue, 3. Plastic deformation, 4. Dent failure and 5. Fatigue failures. Therefore, the probable reasons for the failure in the investigated gearbox might include:

1. Failure due to impact or loads higher than yield stress
2. Dent bending fatigue
3. Damaging corrosion
4. Materials' structural defects
5. Structural defects such as cracks created during heat treatment and machining processes
6. Use of improper materials
7. Design problems
8. Manufacturing process

The general reasons for shaft failure include:

1. Manufacturing process
2. Stress and fatigue
3. Design problems
4. Improper materials
5. Improper maintenance
6. Environmental factors

There are four general reasons for shaft failure which include corrosion, aberration, high loads and fatigue. Corrosion and aberration do not lead to fractures and only cause marks on the shaft that are not capable of breaking the shaft on their own. However, one must consider that corrosion along with fatigue can lead to failure and fracture. Mei Louti Novik et al., [7] investigated failure in manual gearboxes and the reason for creation of pores on gears and corrosion in the gearbox. Parey et al. [8] also in an article investigated failure of air cooled condenser gearbox metallography images.

2 GENERAL CHARACTERISTICS OF GEARBOX

The damaged gearbox had the general dimensions of 2198*01685*760 mm. Table 1 shows the mechanical properties of the investigated gearbox.

Table 1 The mechanical characteristics of gearbox

Mechanical properties	Value	Unit
Ratio	3.722	-
Input speed	1492	rpm
Output speed	400.48	rpm
Motor power	2300	Kw

The transferred power of the gearbox is 2031 KW which is supplied by an engine with the rotational speed of 1492 rpm which is reduced with the ratio of 1/3.72 to the rotational speed of 401 rpm for the compressor and the output torque of 48.4 KN/m. Typical image of a gearbox is shown in Fig. 1; including the investigated gearbox belonged to Arfa Iron and Steel Company and a gear with 67 dents and a pinion with 18 gears. The gear is attached to the compressor using a shaft. The material used in both parts is 17CrNiMo6 alloy.

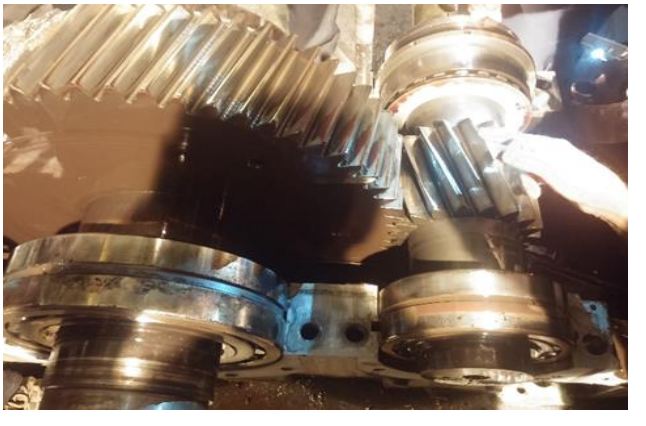

Fig. 1 Typical image of a compressor gearbox

3 CHARACTERISTICS OF DAMAGED PARTS

The damage in the gearbox is seen in two neighboring dents (Fig. 2) and another dent a distance away for the previous ones (Fig. 3). One dent on the pinion and two cracks on the shaft on the attachment point are shown in Figs (4 & 5).

Fig. 2 Two neighbouring damaged dents on the gear

Fig. 3 The lone damaged dent on the gear

Fig. 4 The damaged dent on the pinion

Fig. 5 Damaged location on the shaft

4 ANALYTICAL INVESTIGATION OF DESIGN AND ITS EFFECT ON FRACTURE

In regards to design, three parts are investigated which include gear design, shaft design and keyway and key design.

4.1. Gear design

The data on gear design is as follows:

$$N = 1492rpm\,,\ m_G = 3.72\,,\qquad T = 1300N.M\,,$$
$$P = 2031kw\,,\ \psi = 16.75^\circ\,,\ \phi = 20^\circ\,,\ m_n = 0.620$$

4.1.1. Calculating the necessary width for bending strength

First, the width resulting from bending is calculated and compared to the current value of 155mm.

$$F_{bending} = k_m k_b n_d w_t k_o k_g k_s k_T k_R / m j_p s_t Y_n \tag{1}$$

According to the gearbox design manual:

$$k_b = 1, m = 9, k_m = 1.232, n_d = 0.86,$$
$$k_R = 1.125\ k_0 = k_s = k_T = 1, k_g = 1.117$$

$$W_t = p/v_t \tag{2}$$

$$w_t = 2031000/13.65 = 148791.20N$$

$$J_p = T_J J' \tag{3}$$

The value of the two parameters are:

$$,J' = 0.44[10]\ T_J = 0.93[9]$$
$$S_t = 0.533H_B + 88.3MPa \tag{4}$$
$$H_B = 669.98$$
$$S_t = 445.4MPa$$
$$Y_n = 1.3558N^{-0.0178} \tag{5}$$
$$Y_n = 1.3558(2*10e9)^{-0.0178}$$
$$Y_n = 0.92$$

By using the above equations, we can calculate that appropriate width for bending strength is 122.08mm. Therefore, there is no problem with bending.

4.1.2. Calculating the necessary width for abrasion strength

$$F_w = \left(c_p z_N / s_c k_T k_R\right)^2 n_d w^t k_o k_g k_s k_m c_f / d_p I \tag{6}$$

According to the gearbox design manual:

$$,n_d = 0.86 ,k_\vartheta = 1.117 ,C_f = 1\, C_P = 190MPa$$
$$,w_t = 148791.20N \ ,k_o = k_s = k_t = 1\ k_m = 1.232$$
$$S_c = 2.22H_B + 200MPa \tag{7}$$

$$S_c = 1687.4MPa$$

$$z_N = 2.466N^{-0.056} \tag{8}$$

$$z_N = 0.73$$

$$d_p = m_t n_p \tag{9}$$

$$m_t = m / \cos\psi \tag{10}$$

$$m_t = 9.375$$

$$d_p = 168.75mm$$

$$I = \cos\phi_t \sin\phi_t m_G / 2m_n \left(m_g + 1\right) \tag{11}$$

$$\phi_t = 20.63^\circ$$

$$I = 0.143$$

So:

$$F_w = 38.67mm$$

By using the above equations, we can calculate that appropriate width for wear is 122.08mm. Therefore, there is no problem with wear.

4.1.3. Calculating bending safety coefficient

$$S_F = (S_t Y_N) / (k_T k_R \sigma) \tag{12}$$
$$,S_t = 445.4MPa \ ,K_R = 1.125\ b = 155mm$$
$$,Y_n = 0.92\ K_T = 1$$

Calculating the bending strain in gear and pinion:

$$\sigma = k_H k_b w^t k_o k_\vartheta k_s / Y_J bm_t \tag{13}$$

$$w_t = 148791.2N ,b = 155mm, K_H = 1.232$$

$$m_t = 9.375, K_O = K_S = 1, K_\vartheta = 1.117, Y_{JP} = 0.44$$

$$Y_{JG} = 0.60$$

$$\sigma_P = 320.24MPa, \sigma_G = 251.04MPa$$

So:

$$S_{fp} = 1.02, S_{fG} = 1.4$$

These coefficients show that there is no problem with bending.

4.1.4. Calculating abrasion safety coefficient

$$S_H = S_C Z_N C_H / \sigma_c \tag{14}$$

$$k_T = 1, C_H = 1, Z_N = 1, S_C = 1687.4Mpa, k_R = 1.125$$

$$\sigma_C = \sqrt{W_t k_o k_\vartheta k_s (k_H Z_R / d_{w_1} b z_1) Z_E} \tag{15}$$
$$w_t = 148791.20N , K_o = 1, Z_E = 190MPa, K_\vartheta = 1.117$$
$$K_\vartheta = 1.117, K_{sp} = 0.995, K_{sg} = 1.005, K_H = 1.232$$
$$Z_R = 1, d_{w1} = 168.48mm, b_p = 155mm, b_g = 145mm$$
$$Z_1 = 0.2$$

So:

$$\sigma_{CP} = 1122.80MPa$$
$$\sigma_{Cg} = 1166.69MPa$$

Therefore:

$$S_{HP} = 1.25, S_{HG} = 1.23$$

These coefficients fully meet the initial design requirements. Gear and pinion are suitable in regards to design and strength.

4.2. Gear Shaft design

The initial data and design assumptions include:

$$,R = 99.9\% \ ,M_m = 0kN.m \ \ M_a = 19kN.m$$
$$,K_{fs} = 2.74 \ ,T_m = 24.2KN.m \ ,S_y = 500MPa$$
$$,S_{ut} = 900MPa \ ,T_a = 24.2KN.m \ ,K_f = 1.5$$

The shaft design parameters include:
Modified Goodman equation:

$$d = \left(\frac{16n}{\pi} \left\{ \begin{array}{l} \frac{1}{Se}\left[4\left(k_f M_a\right)^2 + 3\left(k_{fs} T_a\right)^2 \right]^{1/2} + \\ \frac{1}{s_{ut}}\left[4\left(k_f M_m\right)^2 + 3\left(k_{fs} T_m\right)^2 \right]^{1/2} \end{array} \right\} \right)^{1/3} \tag{16}$$

Gerber equation:

$$d = ((8nA)/(\pi S_e)\{1+[1+(2BS_e)/(AS_{ut})^2]^{(1/2)}\})^{(1/3)} \quad (17)$$

$$B = \sqrt{4(k_f M_m)^2 + 3(k_{fs} T_m)} \quad (18)$$

$$A = \sqrt{4(k_f M_a)^2 + 3(k_{fs} T_a)^2} \quad (19)$$

Elliptic equation:

$$d = \left\{\frac{16n}{\pi}\left[4\left(\frac{k_f M_a}{Se}\right)^2 + 3\left(\frac{k_{fs} T_a}{Se}\right) + 4\left(\frac{k_f M_m}{s_{ut}}\right)^2 + 3\left(\frac{k_{fs} T_m}{s_{ut}}\right)^2\right]^{1/2}\right\}^{1/3} \quad (20)$$

Soderberg equation:

$$d = \left(\frac{16n}{\pi}\left\{\frac{1}{Se}\left[4(k_f M_a)^2 + 3(k_{fs} T_a)^2\right]^{1/2} + \frac{1}{s_{ut}}\left[4(k_f M_m)^2 + 3(k_{fs} T_m)^2\right]^{1/2}\right\}\right)^{1/3} \quad (21)$$

According to Fig. 6, the main diameter of the shaft is 200mm and the diameter in keyway is 210mm.

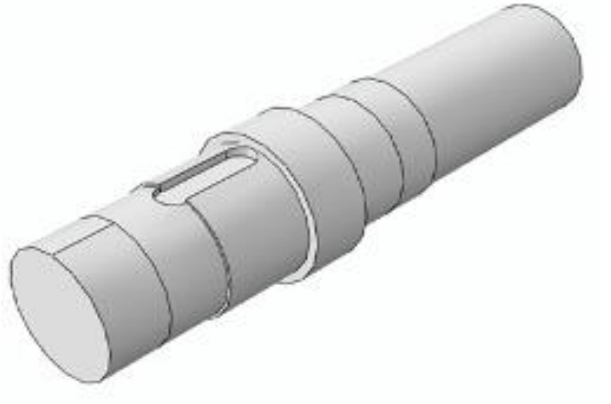

Fig. 6 Three-dimensional map of the gear shaft

Calculation data are presented below:

$$S_e = S_e^{'} k_a k_b k_c k_d k_e K_f \quad (22)$$

$$S_e^{'} = 0.5 S_{ut} \quad (23)$$

$$, k_c = 0.56 \ , k_b = 0.65 \ k_a = 0.744$$
$$, K_f = 1 \ , k_e = 0.753 \ k_d = 1$$
$$S_e^{'} = 450MPa$$
$$S_e = 96.68MPa$$

$$K_f = 1 + (k_t - 1/1 + \sqrt{a/r}) \quad (24)$$

$$k_{fs} = 1 + q_{shear}(k_t - 1) \quad (25)$$

$$, r = 5mm \ , d = 200mm$$
$$r/d = 0.03$$
$$, D = 210mm \ \sqrt{a} = 0.15\sqrt{mm}$$

Two values are calculated for sensitivity coefficient to bending loads and sensitivity coefficient using the following method [11]:

$$k_t = 2, k_{ts} = 1$$
$$q_{shear} = 0.87[12]$$
$$k_f = 1.85, k_{fs} = 1.348$$

The fatigue safety coefficient (n) is equal to 2.32 for each fatigue parameter. Now, gear shaft diameter is calculated using the above equations and shown in table 2.

Table 2 Calculated gear shaft diameter based on different criteria

Criteria	Diameter	Unit
Goodman	220.75	mm
Gerber	221.06	mm
Elliptic	223.13	mm
Soderberg	231.4	mm

Based on standard values and for improved safety, the diameter of 200mm selected for gear shaft is not suitable and the preferred diameter is 240mm.

4.3. Gear shaft key and keyway analysis

The design of keyway is based on the shaft diameter and the material used is normally uniform steel with:

$$S_y = 370MPa, S_{sy} = 215MPa$$

The changing parameter in the shaft is its length. Since stress concentration on the keyway is high on the shaft, proper care should be taken in its design.

4.3.1. Calculating shaft diameter at keyway using different criteria

The dimensions of the current key are 50*28*110mm. Since the damaged gear was not yet dismantled, it was not possible to measure the diameter of keyway but pictures of the previous gearbox show that the diameter

is less than 4mm (r/d<0.02) which leads to stress concentration coefficients of:

$$K_t = 2.14, K_{ts} = 3[13]$$

Based on the equations presented in shaft design section and using these coefficients, shaft diameter is calculated and shown in table 3.

Table 3 Gear shaft diameter at keyway based on different criteria

Criteria	Diameter	Unit
Goodman	258.06	mm
Gerber	221.31	mm
Elliptic	251.52	mm
Soderberg	263.97	mm

Therefore, the shaft diameter at keyway should be 270mm instead of 210mm.

4.3.2. New key and keyway design

The length of the key should be designed based on compression and shear stress. Here, since the length of the key is known (110mm), the safety coefficients for these two conditions are controlled. Fig. 7 shows key parameters.

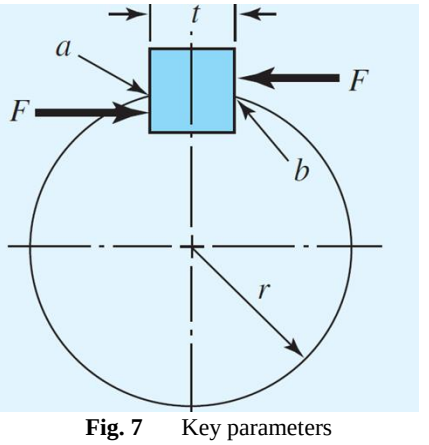

Fig. 7 Key parameters

The new key will have the dimensions of 63*32*110mm [14]. It is worth noting that the depth of keyway on the shaft is 20mm and 12mm of the key is inside of the keyway.

Calculating the reliability coefficient:

$$d = 240mm, P = 2031kw, T = 41.4kn.m$$
$$F = T / r \quad (26)$$
$$F = 403kN$$

Compression:

$$n = s_{sy} tl / F \quad (27)$$

$$n = 3.6$$

Shear:

$$n = s_{sy} hl / F \quad (28)$$

$$n = 1.2$$

The maximum length of the key is 118mm and here the length of110mm was selected.

5 INVESTIGATING THE REASON FOR FRACTURE USING FRACTURE STUDIES

The fracture surfaces of the gear were investigated as shown in Fig. 8 in order to determine the reason for failure.

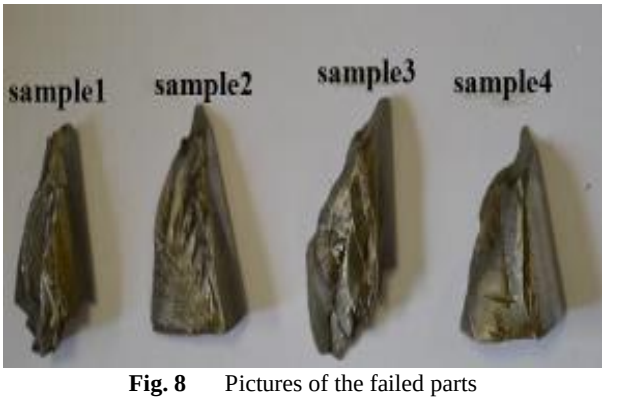

Fig. 8 Pictures of the failed parts

In order to investigate the fracture surface, the initial investigation was started using normal stereomicroscope and continued using Scanning Electron Microscope (SEM) method.

5.1. Microscopic studies

During the visual investigation of the fractured samples, it was determined that all samples were fractured at two-third of the height from dents' base (Fig. 9), which is the location with the highest shear stress.

The surfaces of the samples also show signs of overheating as changes in color which could have happened during operation due to insufficient lubrication or due to misalignment. Overheating can lead to creation of residual stress and changes in surface structure and facilitates the formation of cracks.

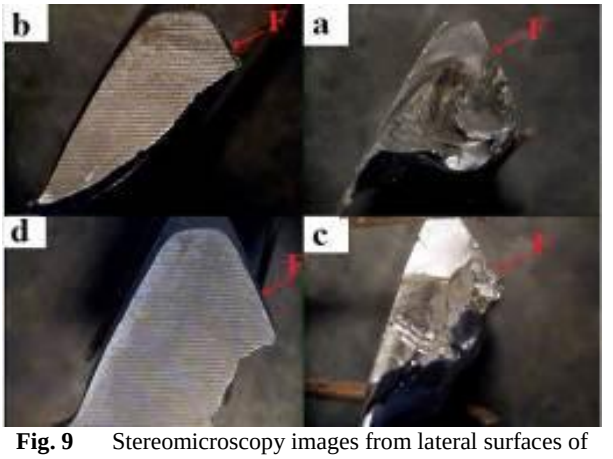

Fig. 9 Stereomicroscopy images from lateral surfaces of the samples and the direction of the forces on a-d gears for samples 1 to 4

The signs of discoloration due to overheating on the samples' surfaces can be seen in Fig. 10. This discoloration was more intense and varied in sample 4 while it was less varied in sample 2. Only in samples 1 and 3, the signs of overheating are seen on the surface where the fracture has started.

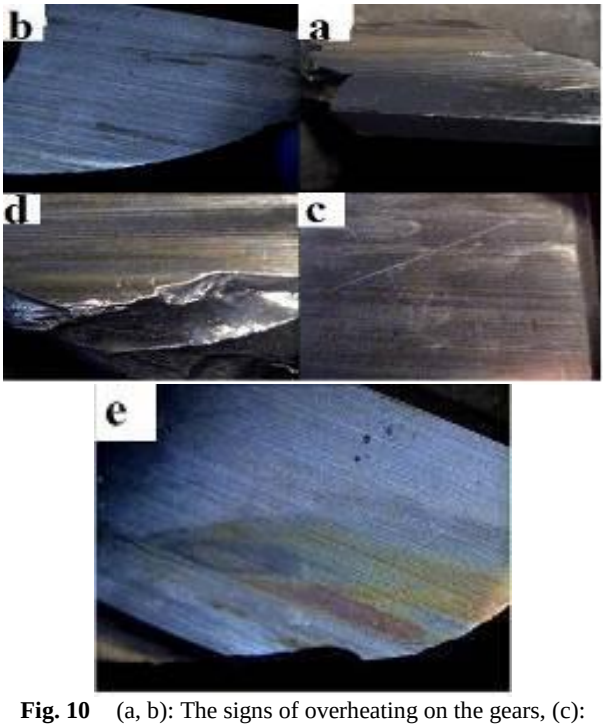

Fig. 10 (a, b): The signs of overheating on the gears, (c): variety of signs in sample 1, (d): variety of signs in sample 2, (e): variety of signs in sample 4

The study of the fracture surfaces showed that all samples except sample 3 have wave-like fracture surfaces which shows an unstable growth of cracks due to sudden impact force while the changes in the waves' directions shows the growth directions of the cracks. These lines show significant plastic deformation. The stress concentration points and starting locations of the cracks are shown in figures with red cycles. The images show that plastic deformation is higher in samples 1 and 2 and has happened since the start of the fracture which shows the presence of a high load. Stereomicroscopy image of sample 1 and sample 2 are shown in Figs. 11 and 12, respectively. Based on the fracture in samples 3 and 4 and comparing the surfaces of the gears, it can be said that samples 3 and 4 are the first to fail and samples 1 and 2 are the final fracture surfaces. For this reason, fracture surfaces in samples 3 and 4 were selected for further studies. Also the Stereomicroscopy image of sample 3 and sample 4 are shown in Figs. 13 and 14, respectively.

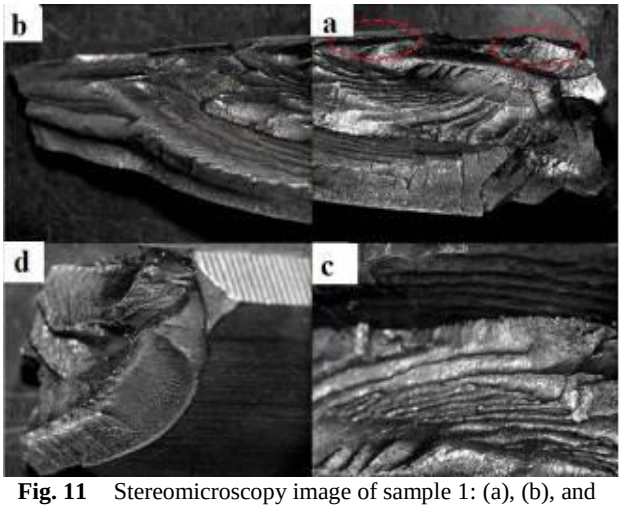

Fig. 11 Stereomicroscopy image of sample 1: (a), (b), and (c): wave-like fracture and (d): brittle fracture on the lateral surface of the gear

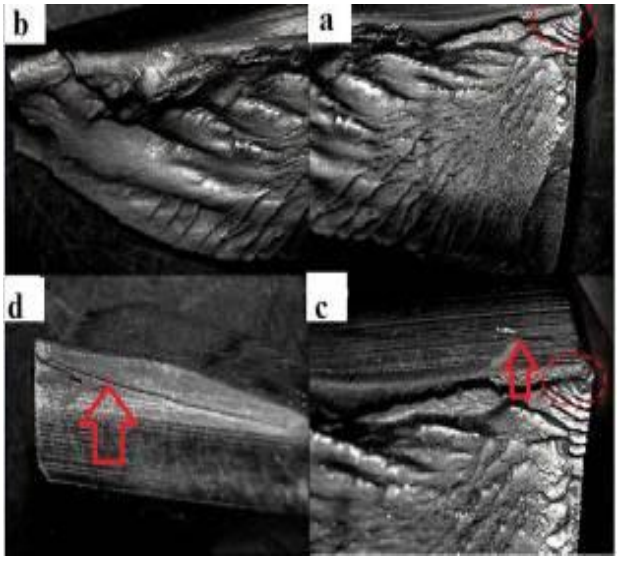

Fig. 12 (a, b): Stereomicroscopy image of wave-like fracture and (d, c): cracks: in sample 2

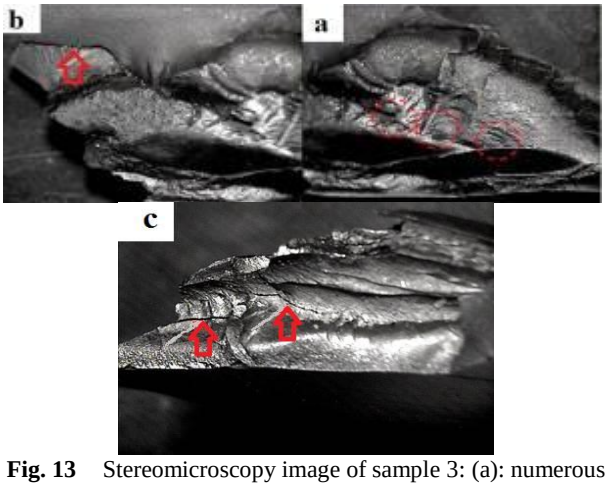

Fig. 13 Stereomicroscopy image of sample 3: (a): numerous points of stress concentration, (b) and (c): cracks under the surface and at the center of the sample

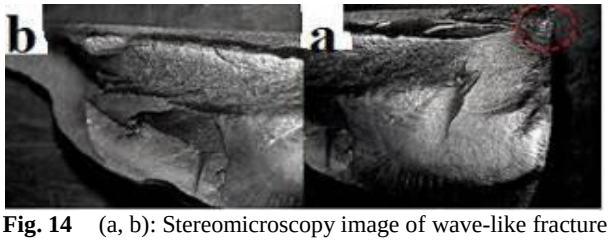

Fig. 14 (a, b): Stereomicroscopy image of wave-like fracture sample 4

5.2. Scanning Electron Microspore (SEM) studies

The supplementary fracture studies were carried out using SEM method. To this end, the surface of sample 3 was investigated at two locations of fracture's start and center of the gear and it was determined that all fractures are brittle and from grain boundary type. The fracture regions are shown in Fig. 15. A large part of the fracture at the center of the sample was damaged due to abrasion but investigating the intact parts showed that there are numerous cracks at the center and under the surface which might have structural sources. There were also traces of impact on the sample's surface which can be the reason for expansion of cracks and final fracture. SEM images of outside and center of the sample 3 are demonstrated in Figs. 16 and 17, respectively.

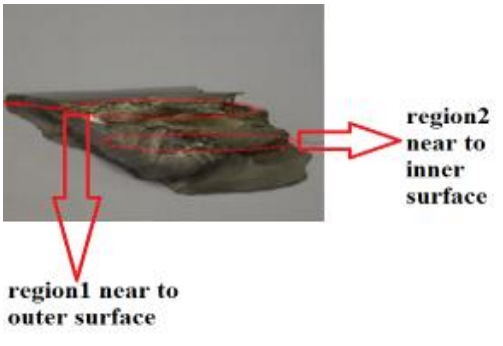

Fig. 15 Investigated locations using SEM in sample 3

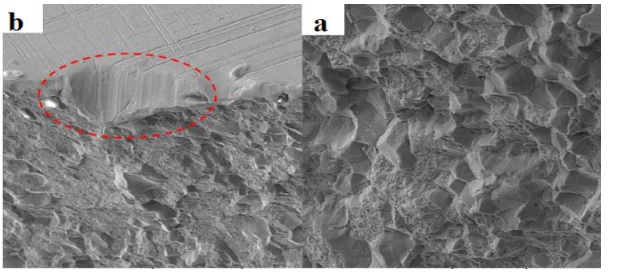

Fig. 16 SEM image of brittle grain boundary fracture near the surface of sample 3 and traces of impact on the outside surface

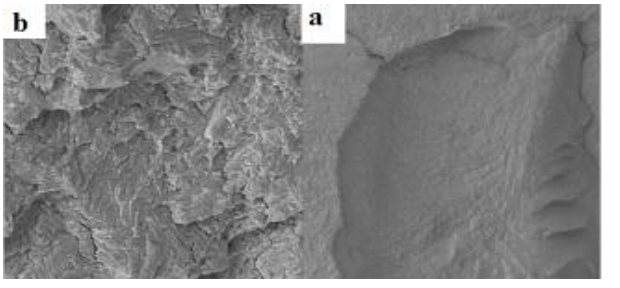

Fig. 17 SEM images of brittle fracture and cracks at the center of sample 3

Investigating sample 4 at the start of the fracture and at the gear's center showed that the fracture surface is a mixture of soft and brittle fractures. Its fracture regions are shown in Fig. 18. The edges leading to the outside surface show brittle grain boundary fracture while the center of the sample showed soft fracture. It is worth noting that in fractures resulting from sudden application of force, it is possible to see a mixture of soft and brittle fractures simultaneously. SEM images of outside and center of the sample 4 are demonstrated in Figs. 19 and 20, respectively. This characteristic of fracture surface can also be due to microscopic differences between surface and center of the gear in which harder surfaces show increased brittle fracture while at the center fracture is often soft. A large part of the fracture surface at the center was unrecognizable due to abrasion.

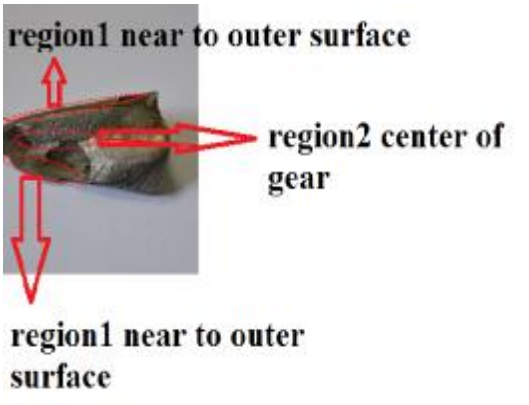

Fig. 18 Investigated Locations using SEM in sample 4

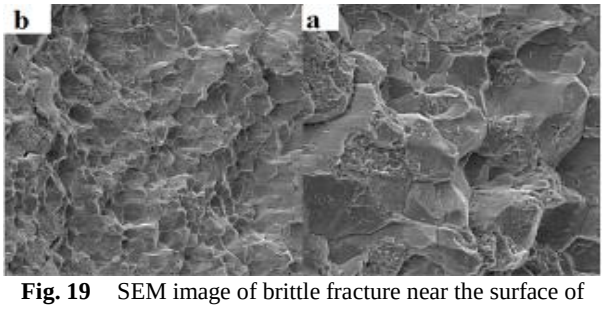

Fig. 19 SEM image of brittle fracture near the surface of sample 4

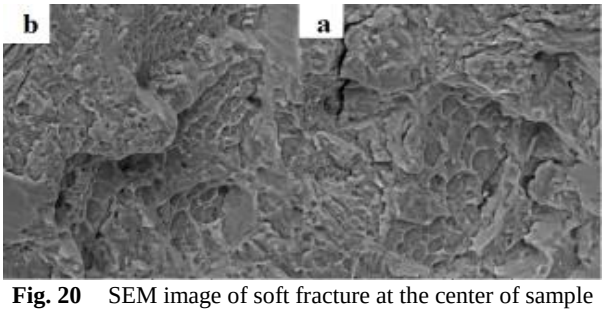

Fig. 20 SEM image of soft fracture at the center of sample

6 SOFTWARE SIMULATION

6.1. Stress analysis for gear shaft

The results of the analysis were used to redesign a new shaft. The goal of stress analysis is to investigate the strength of the structure under maximum load and also to identify critical stress concentration points in the designed structure. These results are used to make the necessary corrections in the initial shaft design. 3d models of old shaft and redesigned shaft are shown in Fig. 21.

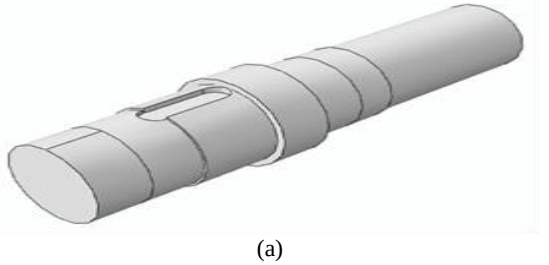

(a)

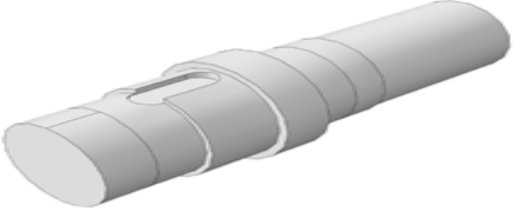

(b)

Fig. 21 3D model of (a) old shaft (shaft No. 1), (b) the redesigned shaft (Shaft No. 2)

6.1.1. Modeling and mechanical characteristics

The material's properties including its elasticity modulus of 200 GPa and Poisson coefficient of 0.3 are used in the modeling. The analysis type is static analysis.

6.1.2. Border conditions and loading

The shaft is tethered in the radial direction at the location of bearings, in the rotational direction (θ) at the compressor's location (loading location) and in the longitudinal direction at the bearing support in the middle of the shaft. The rotational torque applied to the shaft using gear's key is applied as expanded compression loading on the keyway. Therefore, the force w_t is distributed on the cross section of the keyway and is applied as a compression force on the keyway's wall in ABAQUS software (Fig. 22).

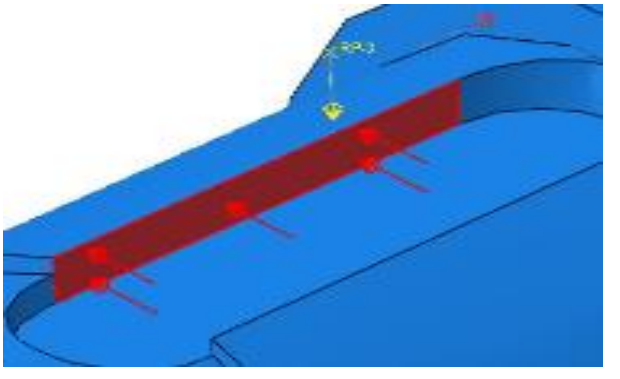

Fig. 22 Force applied at the keyway's wall in shaft 1 and 2

The lateral force applied from pinion to the shaft, W_r, is applied to the upper surface of the shaft at the location of the gear as a concentrated force (Fig. 23). Since solid elements are not capable of handling concentrated forces, a reference point is used for this force.

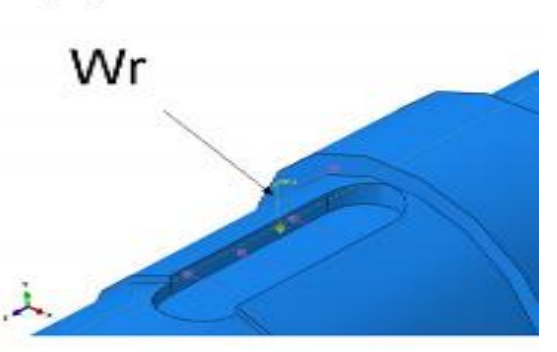

Fig. 23 Radial loading for shaft 1 and 2

The longitudinal force applied by the pinion to the shaft, W_a, is tolerated by the outer ring of the middle bearing and is applied as a compression force similar to W_t on the support bridge of the hear (Fig. 24).

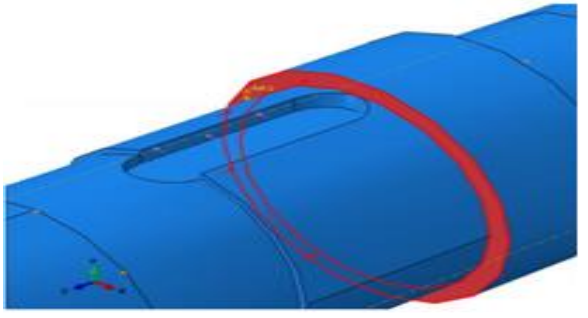

Fig. 24 The longitudinal force applied from pinion to shaft 1 and 2

6.1.3. Shaft meshing

The type of element used in finite element analysis of this problem is a solid, three-dimensional and tetrahedron type element called C3D10 element with 10 nodes. The schematic of this element is seen in Fig. 25.

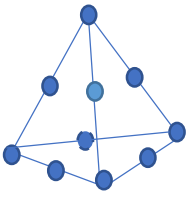

Fig. 25 The element used in finite element analysis of shaft

The proper size of elements is determined using meshing studies. To this end, the point shown in Fig. 26 is selected and the size of elements close to that point is changed and model's stress analysis is repeated after each change. By drawing the graph of stress that the selected point versus the size of elements, the dependence of results on meshing is determined. The selected point is located at the stress concentration location.

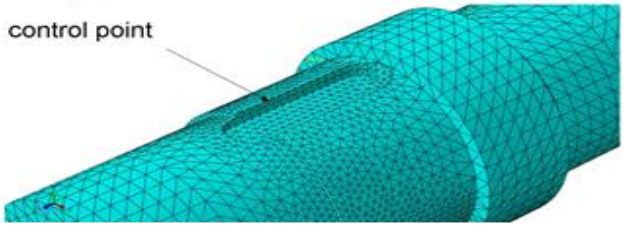

Fig. 26 The selected point for stress analysis

The results of meshing study are shown in table 4 and Fig. 27. Based on these results, the size of 14 millimeters is suitable for elements because using elements smaller than 14 mm leads to no significant changes in the results.

6.1.4. Shaft stress analysis results

The von Mises stress for shaft 1 is shown in Fig. 27. According to the results, the maximum stress occurs at the edge of the keyway (area 1). We can also clearly see that after the edge of the keyway, maximum stress locations include the half-cycle near gear's support bridge (area 2) and the step near the bearing (area 3). It is necessary to mention that cracks in the shaft (Fig. 28) show the presence of maximum stress at these locations and therefore confirm the results of finite element analysis.

Table 4 The characteristics of the investigated point.

Mesh size (mm)	Number of elements	Number of nods	Stress at the selected point (MPa)
8	89364	127216	145.4
10	67683	96954	147.8
12	54114	78086	148.3
15	44766	64981	146.9
17	42075	61204	148
20	40780	59399	139.6

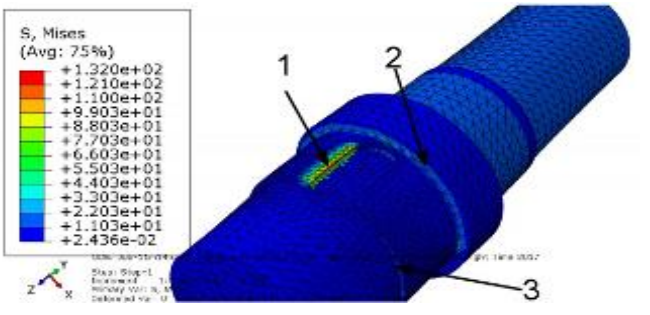

Fig. 27 Von Mises stress for shaft 1

Fig. 28 The fractured gear shaft

Afterwards, the redesigned shaft was analyzed using ABAQUS software. The results showed that despite improved stress distribution in the entire shaft and at locations near keyway (Figs. 29a and 29b), maximum stress has increased due to sudden change in area and creation of sharp edges at the location of the keyway.

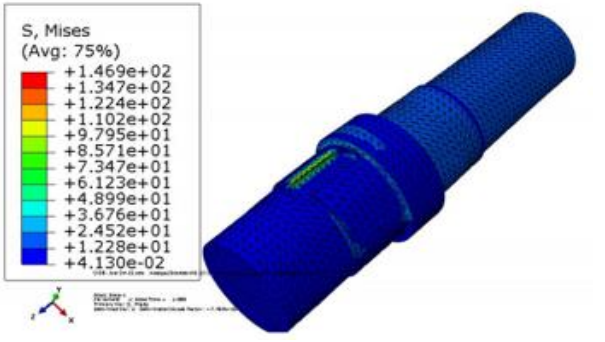

(a)

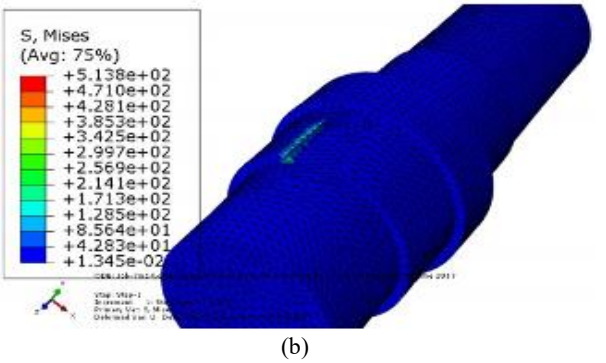

(b)

Fig. 29 Stress distribution in (a) shaft 1 and (b) shaft 2

Therefore, based on these results and in the allowed range determined using design calculations, shaft diameter is modified in two stages until the problem is solved. The suitable diameter determined from repeated stress analyses is 251 mm. the results of the final shaft design is shown in Fig. 30. As can be seen, in this shaft, both the stress distribution and maximum stress are reduced.

Fig. 30 Stress distribution in redesigned shaft 2

6.2. Key stress analysis

The three-dimensional models of old and redesigned keys are shown in Fig. 31.

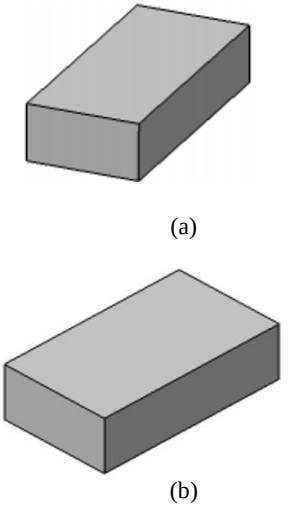

(a)

(b)

Fig. 31 Three-dimensional model of (a) key 1 and (b) key 2

6.2.1. Border conditions and loading of keys 1 and 2

The border locations applied to the key is as follows:
The side of the key that touches the keyway is tethered at the direction of shaft's radios (y axis, Fig. 32).

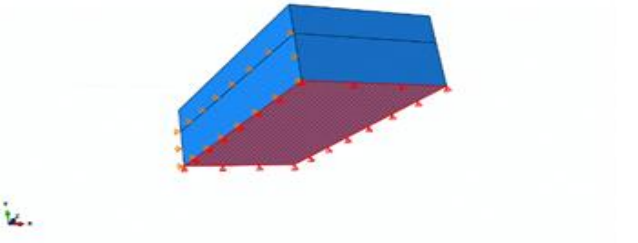

Fig. 32 Tethering of key's bottom for key 1 and 2

The part of key's side which transfers rotational torque to the shaft (Fig. 33) is tethered at the direction of x axis.

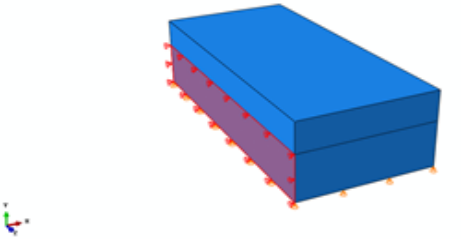

Fig. 33 The tether of side of key 1 and 2

The loadings are as follows:
The rotational torque applied to the shaft is applied as an expanded load to part of the key's wall from the wall of gear's keyway as a result of W_t force. This force is applied as a compression force due to being divided by the cross-section of keys 1 and 2 (Fig. 34).

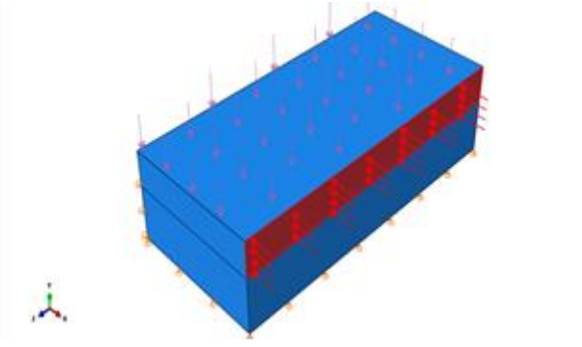

Fig. 34 The force applied on the wall of key 1 and 2

The force W_r is applied from gear to the key (Fig. 35). This force is directly applied to the cross-section of key 1 and 2 as a compression force.

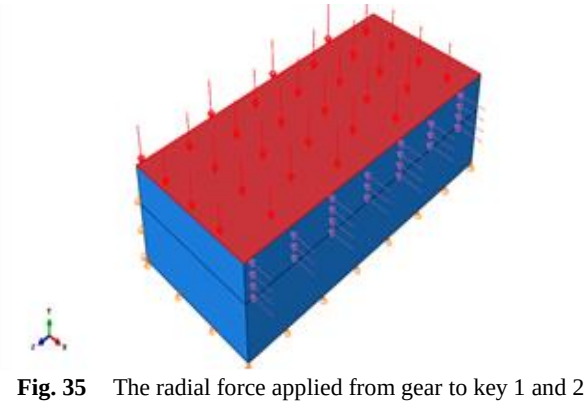

Fig. 35 The radial force applied from gear to key 1 and 2

6.2.2. Key meshing

Given the simple geometry of the key, the best element used for static stress analysis of the key is a hexagonal element applied to the key.

The element type used in finite element analysis is a solid, linear and hexagonal element called C3D8R element with 8 nodes. The schematic of this element is shown in Fig. 36.

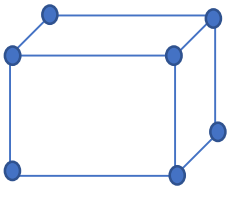

Fig. 36 The element used for finite element analysis of keys 1 and 2

6.2.3. Key stress analysis result

The results of stress analysis for key 1 and 2 are shown in Fig. 37.

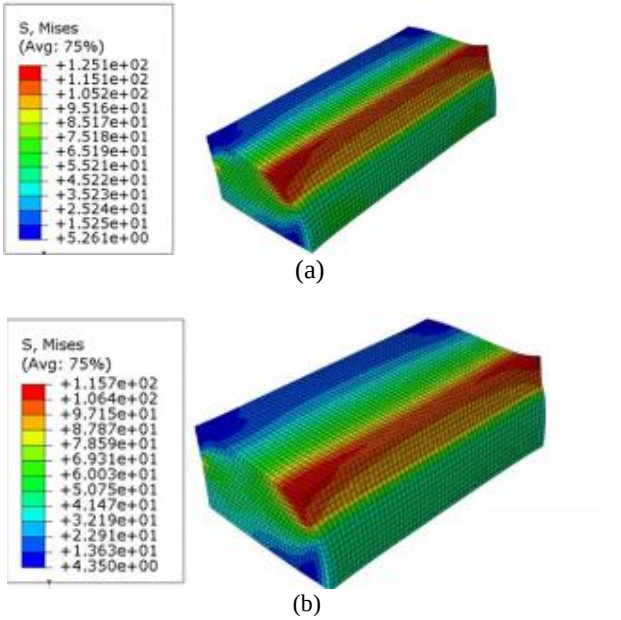

Fig. 37 Stress distribution in: (a): key 1 and (b): key 2

7 CONCLUSIONS

7.1. Analytical investigation

Investigating the gearbox showed proper design in gears but intense stress concentration at the location of keyway, due to small diameter. In other words, the shaft diameter should be 270mm. while main shaft diameter was 240mm. Investigating the design of the key revealed its excessive length which led to a safety coefficient of 1.3 and lack of fracture.

Based on these facts, it can be concluded that fatigue caused by more than one million cycles has led to creation and expansion of cracks on the stress concentration locations (keyway and the location with different shaft diameter, Figs. 38 and 39). Since the length of the key was longer than necessary, instead of damaging to the key, the shaft has been damaged which had led to the fracture. The creation and expansion of cracks on the shaft has led to misalignment of gears with each other, leading to abrasion and finally fracture.

Fig. 38 Cracks at stress concentration points of the diameter change location

Fig. 39 Crack expansion from stress concentration points in the keyway

7.2. Fracture studies

Based on the results of analysis of the fracture and based on the wave-like formations at fracture start points in samples 1, 2 and 4, there has been considerable plastic deformation due to high loads and these three gears have failed due to excessive load. In the gear 3, the presence of small cracks on the structure shows that high load has led to fracture and deformations of the gear. There is no plastic deformation resulting from high loads in this sample due to expansion of the cracks.

7.3. Software result

According to software results, it can be said that the suitable diameter size of the shaft is 251 mm. The model shows that maximum stress in this new design is lower than the initial value and also has a better distribution.

REFERENCES

[1] Panwar, V., Mogal, S., A Case Study on Various Defects Found in a Gear System, International Research Journal of Engineering and Technology, Vol. 3, No. 3, 2015, pp. 425- 429.

[2] patel, J., Sahu, G., Sen, P., A Study on Common Failures of Gears, International Research Journal of Engineering and Technology, Vol. 2, No. 6, 2015, pp. 301- 307.

[3] Pandhal, D. K., Meshram, D. B., Analysis and Failure Improvement of Shaft of Gear Motor in CRM Shop, International Journal of Engineering and Science, Vol. 3, No. 4, 2013, pp. 17- 24.

[4] Lanzutti, A., Gagliardi, A., Raffaelli, A., Simonato, M., Furlanetto, R., Magnan, M., Andreatta, F., and Fedrizzi, L., Failure Analysis of Gears, Shafts and Keys of Centrifugal Washers Failed During Life Test, Engineering Failure Analysis, Vol. 79, No. 3, 2017, pp. 634-641.

[5] Yucel, S., Ozenli, L., Gencol, T., and Alanyalı, E., Flywheel Starter Ring Gear Failures and Hardness Variation Reduction in Surface Hardening Process, Engineering Failure Analysis, Vol. 4, 2015, pp. 8-19.

[6] Rossino, L., Castro, D., Moreto, J., Ruchert, C., pinelli, S., and Trapani, J., Surface Contact Fatigue of a Case-Hardened Pinion Shaft, Material Research, Vol. 3, No. 17, 2014, pp. 535- 541.

[7] Milutinovic, M., Trifkovic, S., Duric, A., and Vucetic, N., Gear Failures Embedded in Manual Gearboxes, Bulletin of Engineering, Vol. 1, No. 1, 2016, pp. 83- 84.

[8] Parey, A., Jain, N. K., Gencol, T., and Koria, S. C, Failure Analysis of Air Cooled Condenser Gearbox, Engineering Failure Analysis, Vol. 2, 2014, pp. 150-156.

[9] Shadravan, E., Mechanical Engineering Design, 9rd ed., Nopardazan, IRAN, 2011, pp. 780.

[10] Shadravan, E., Mechanical Engineering Design, 9nd ed., Nopardazan, IRAN, 2011, pp. 779.

[11] Peterson, R., Pilkey, W., and Pilkey, D., Stress Concentration Factors, 3rd ed., Wiley, New York, 2008, pp. 165-167.

[12] Shadravan, E., Mechanical Engineering Design, 9rd ed., Nopardazan, IRAN, 2011, pp. 309.

[13] Shadravan, E., Mechanical Engineering Design, 9rd ed., Nopardazan, IRAN, 2011, pp. 388.

[14] Valenejad, A., Tables and Standards in Design and Machine, 1nd ed., Tarrah, IRAN, 2009, pp. 241.